

Received: 2022.04.15
Accepted: 2022.05.24
Available online: 2022.06.01
Published: 2022.06.23

Expression of the *GZMB* Gene Polymorphism, SNP rs8192917, in 990 Han Chinese Patients with Postoperative Keloids

Authors' Contribution:
Study Design A
Data Collection B
Statistical Analysis C
Data Interpretation D
Manuscript Preparation E
Literature Search F
Funds Collection G

CDE 1,2 **Xiulin Wen**
BF 1 **Huicong Du**
BF 1 **Xiaoyan Hao**
BF 3 **Jingrong Wang**
AG 1 **Yuan Guo**

1 Department of Plastic, Aesthetic and Maxillofacial Surgery, The First Affiliated Hospital of Xi'an Jiaotong University, Xi'an, Shaanxi, PR China
2 Department of Nursing, The First Affiliated Hospital of Xi'an Jiaotong University, Xi'an, Shaanxi, PR China
3 Department of Nursing, College of Nursing, Shaanxi University of Chinese Medicine, Xianyang, Shaanxi, PR China

Corresponding Author:

Financial support:

Conflict of interest:

This research was totally supported by the Key Research and Development Program of Shaanxi (No.2020SF-224)

Yuan Guo, e-mail: yuanguoxa@163.com

None declared

None declared

Background: A keloid is a pathological scar hyperplasia that is affected by genetic and environmental factors. Although the involvement of cytotoxic granzyme B in keloids has been recognized, there is almost no research on granzyme B (*GZMB*) gene polymorphisms and keloids. This study aimed to explore the relationship between genetic polymorphisms of *GZMB* and postsurgical keloid susceptibility in the Han Chinese population.

Material/Methods: A total of 3078 participants, including 990 patients with postsurgical keloids and 2088 controls without postsurgical keloids, were enrolled. We selected 15 common DNA variants in the *GZMB* gene for analysis. Associations were analyzed in both single marker-based and haplotype-based methods. The Genotype-Tissue Expression database was used to examine the biological significance of the targeted single nucleotide polymorphisms (SNPs).

Results: SNP rs8192917 was found to be associated with the susceptibility of keloids (t statistic=4.82, $P=1.47 \times 10^{-6}$). An increased risk of keloids was significantly associated with the minor allele (C allele) of rs8192917 (odds ratio=1.33; 95% CI=1.18-1.49], $P=1.47 \times 10^{-6}$). In addition, a significant association was reported for genotypes of rs8192917 and clinical severity of keloids ($\chi^2=10.61$, $P=0.03$).

Conclusions: The results suggested there are significant associations between common genetic variants in *GZMB* and the susceptibility of postsurgical keloids in the Chinese Han population. These genetic polymorphisms were also related with the severity of postsurgical keloid symptoms in participants with keloids. The current study can contribute to future etiological and clinical research of keloids.

Keywords: **Case-Control Studies • Disease Susceptibility • Keloid • Polymorphism, Single Nucleotide**

Full-text PDF: <https://www.medscimonit.com/abstract/index/idArt/936963>

 2688

 6

 4

 41



Background

Keloid and hypertrophic scars represent an aberrant response to the wound healing process [1]. These scars are caused by cutaneous injuries, such as trauma, burns, surgeries, or uncertain origins, which is different from the origins of other scar types. Keloids are clinically treated as a benign skin tumor [2], and their incidence in the Asian population can be as high as 4% to 16% [3]. Keloid tissue is usually accompanied by chronic inflammation, and it is prone to infection and ulceration, which can lead to scar carcinoma [4,5]. Furthermore, for keloids, the prognosis of squamous cell carcinoma is poor and mortality is high [6]. Keloids can occur in locations including the ears, chin, chest, back, and vulva and are accompanied by unbearable itching and tingling and a serious negative impact on the quality of life and mental state of patients [7,8]. Due to the unclear pathogenesis of keloids, they have always posed a difficult problem in the field of plastic surgery.

There are currently many hypotheses about the formation of keloids, such as the immunology, tension, and endocrine hypotheses. Early studies have found that compared with in normal tissues, the concentrations of T lymphocytes, B lymphocytes, macrophages, and immune complexes in the peripheral circulation of keloids are significantly increased, and it is speculated that the proliferation of keloids may be caused by immune stimulation [9,10]. Genetic and molecular epidemiologic studies have suggested that the polymorphisms of many genes that affect the proliferation and apoptosis of keloid fibroblasts or extracellular deposition and degradation are associated with keloid risk, including TGF- β , Bcl-2, Smad7, IL-6, IL-4, IL-10, and Fas [11,12]. TGF- β is recognized as one of the most representative cytokines closely related to wound healing [13]. Given that hyperproliferation of fibroblasts is a major feature of keloids and that inflammation is associated with poor prognosis, the Fas/FasL pathway, which plays an important role in cell apoptosis, is thought to be associated with keloids. Some single nucleotide polymorphism (SNP) sites in exons 7 to 9 of the *Fas* gene are very likely to be related to functional changes in the Fas protein, leading to the formation of local keloids [14,15].

The cytotoxic granzyme B (GzmB)/perforin pathway shows a similar function to the Fas/FasL pathway in apoptosis and inflammation, leading to poor healing of damaged tissues. There are 5 granzymes in humans, of which granzyme B is a serine protease encoded by the *GZMB* gene (located at 14q12) that is mainly secreted by natural killer cells, CD8⁺ T lymphocytes (CTLs), and tumor cells. It can induce the expression of inflammatory factors and promote tissue fibrosis by releasing TGF- β , activating interleukin, and degrading decorin [16]. Therefore, granzyme B is thought to be involved in inflammatory skin diseases [17]. Research has observed decreased

decorin levels in keloid scar tissue compared with in normal skin, while reduced decorin is associated with collagen disorders in animal models, and *GzmB* knockout could inhibit this phenomenon to some extent [18,19]. Consistently, another report demonstrated that using *GzmB* inhibitors can also speed up wound healing [20]. However, *GzmB* appeared to have no physiological function in healthy *GzmB*-knockout mice or in young, healthy human skin [21,22]. Although 2 gene association mapping studies have been published on keloids [23,24], there is almost no research focused on *GZMB* gene polymorphisms. As basic patient characteristics, such as age, sex, and recurrence history, can play an important role in keloid treatment, there is an urgent need for more efficacious options.

To date, no study in Han Chinese individuals examining the association of the *GZMB* gene with postsurgical keloids is available. Thus, our study aimed to explore the correlation between the *GZMB* gene and postsurgical keloid genetic susceptibility in the Chinese Han population based on a candidate gene association mapping study design to provide more insights into the etiology of keloids.

Material and Methods

Ethics Statement

Written informed consent was obtained from all participants. This study was approved by the Ethics Committee of the First Affiliated Hospital of Xi'an Jiaotong University per reference 20171016YG dated October 18, 2017, and the study procedures were performed following the tenets of the Declaration of Helsinki (version 2002).

Study Participants

A total of 3078 study participants, including 990 patients with postsurgical keloids and 2088 control participants without postsurgical keloids, were consecutively recruited from the Plastic and Aesthetic Surgery Outpatient Department of the First Affiliated Hospital of Xi'an Jiaotong University between Jan 2018 and July 2021. All participants were unrelated Han Chinese individuals (at least 3 generations were of Han descent and had no history of migration). All participants were examined carefully by at least 2 dermatologists. According to the shape of the scars, proliferation outside the original wound boundary, and invasion of the surrounding normal skin, keloids were diagnosed. The diagnosis of the hypertrophic scar was confirmed when the height of the scar was more than 2 mm above the normal surrounding skin [25]. Patients with hypertrophic scars and some keloid syndromes were excluded from the study. The severity of keloids was assessed according to color, scar height, pliability, pain, and itching of keloid

Table 1. Characteristic and demographic information of the study participants.

| Variables | Cases (N=990) | Controls (N=2,088) | Statistics | P |
|-----------------------|---------------|--------------------|-----------------|------|
| Age, mean±sd | 40.3±15.0 | 40.3±17.2 | t=-0.11 | 0.91 |
| Gender (%) | | | | |
| Male | 584 (59) | 1,234 (59) | | |
| Female | 406 (41) | 854 (41) | $\chi^2=0.0003$ | 0.99 |
| Family History (%) | | | | |
| Yes | 121 (12) | 246 (12) | | |
| No | 869 (88) | 1,842 (88) | $\chi^2=0.0857$ | 0.77 |
| Clinical Severity (%) | | | | |
| Mild | 273 (28) | – | | |
| Moderate | 503 (51) | – | | |
| Severe | 214 (21) | – | – | – |

scars [26]. All healthy controls without keloids were from the same clinics, and all participants were free of obesity and autoimmune and systemic diseases in the study. Peripheral blood samples were collected from the study participants and preserved for further genotyping experiments. Demographic information, including age, sex, and family history of the study participants, was collected from questionnaires and medical records and is presented in **Table 1**.

SNP Choice and Experiment for Genotyping

GZMB is a short gene of only approximately 3.2 kb that includes untranslated regions. We extracted all common DNA variants (MAF ≥ 0.05) from the gene region based on data from the 1000 Genomes Project. We selected a total of 15 SNPs for genotyping (**Supplementary Table 1**). Genomic DNA was extracted using a commercial DNA kit (Axygen Scientific Inc, Union City, CA, USA). The candidate SNPs were genotyped based on the Sequenom MassARRAY platform, and the raw data were processed by a Typer Analyzer. Labels of samples (cases or controls) were blinded to technicians performing the genotyping experiments. Five percent of the study samples were replicated for genotyping experiments, and a 100% concordance rate was achieved.

Statistical Methods

Power analysis was conducted using the GAS genetic power calculator (https://csg.sph.umich.edu/abecasis/gas_power_calculator/), and the result is summarized in **Supplementary Figure 1**. Characteristic and demographic variables were observed between participants with keloids and healthy controls. Genotyping quality was estimated by Hardy-Weinberg equilibrium tests conducted in the control group. Logit models were applied to each genetic marker for examining the association signals between genotypes and susceptibility to keloids. In the

logistic model, the genotypes of each SNP were coded in additive mode. For 0, 1, or 2 copies of the minor allele, the SNP was coded as 0, 1, or 2. Plink [27] was utilized for fitting logistic models. Multiple testing was addressed by Bonferroni corrections through which the threshold *P* value was determined by 0.05 divided by the number of tests. Linkage disequilibrium (LD) patterns were analyzed using Haploview [28]. The standard method was applied to constructing LD blocks based on our genotyped SNPs [29]. Haplotypic frequencies in participants with keloids and controls were estimated and compared to identify significant haplotypes related to risk of keloids. In addition to the susceptibility to keloids, the relationship between genotypes of targeted SNPs and the clinical features of keloids were also investigated. The statistical computing program R was used for descriptive and general statistical analyses.

Methods for In Silico Analyses

In silico analyses were performed to investigate the biological significance of the top hit association signals identified in the association analyses. Several bioinformatics tools and databases were utilized. SIFT [30] and polyphen2 [31] were used to examine the biological significance of nonsynonymous variants on protein structures. The Genotype-Tissue Expression database was used to depict the potential expression quantitative trait loci (eQTL) pattern for candidate genes in various kinds of human tissues [32].

Results

Demographic Characteristics of the Participants

With the formation of dermal hyalinized collagens visible under a microscope, keloids are seen to expand beyond the

Table 2. Results of the single marker-based association analyses.

| CHR | SNP | BP | A1 | OR [95%CI] | T-statistics | P |
|-----------|------------------|-----------------|----------|-------------------------|--------------|-----------------------------|
| 14 | rs2236337 | 24631041 | C | 0.89 [0.79-1.00] | -2.00 | 0.05 |
| 14 | rs2236338 | 24631076 | G | 1.13 [1.27-2.03] | 2.04 | 0.04 |
| 14 | rs74345106 | 24631185 | T | 0.87 [0.59-1.27] | -0.73 | 0.46 |
| 14 | rs6573910 | 24631676 | T | 0.89 [0.79-1.00] | -1.98 | 0.05 |
| 14 | rs6573911 | 24631727 | T | 1.13 [1.01-1.26] | 2.09 | 0.04 |
| 14 | rs71405867 | 24632191 | G | 1.03 [0.90-1.19] | 0.43 | 0.66 |
| 14 | rs1126639 | 24632342 | A | 0.89 [0.79-1.00] | -1.99 | 0.05 |
| 14 | rs11539752 | 24632383 | C | 0.88 [0.78-1.00] | -2.01 | 0.04 |
| 14 | rs10909625 | 24632423 | C | 1.13 [1.01-1.27] | 2.08 | 0.04 |
| 14 | rs10873219 | 24632500 | T | 1.03 [0.90-1.18] | 0.41 | 0.69 |
| 14 | rs59268439 | 24632691 | T | 0.94 [0.80-1.11] | -0.70 | 0.48 |
| 14 | rs9671454 | 24632850 | C | 0.90 [0.69-1.19] | -0.74 | 0.46 |
| 14 | rs8192917 | 24632954 | C | 1.33 [1.18-1.49] | 4.82 | 1.47×10⁻⁶ |
| 14 | rs2273843 | 24634203 | C | 1.04 [0.90-1.20] | 0.49 | 0.63 |
| 14 | rs2273844 | 24634208 | A | 1.03 [0.92-1.16] | 0.55 | 0.58 |

CHR – chromosome; A1 – tested allele; BP – number of patients with keloids in different genotype groups; UNAFF – number of controls in different genotype groups. OR [95% CI] – odds ratio with 95% confidence interval. Significant results are highlighted in bold.

boundaries of the initial lesions. Hypertrophic scars, on the other hand, tend to form within the limits of wounds and present histologically as dermal nodules (**Supplementary Figure 2**). A total of 3078 participants, including 990 patients with keloids and 2088 healthy controls, were enrolled in this study. No significant differences were identified for age ($t=-0.11$, $P=0.91$), sex ($\chi^2=0.0003$, $P=0.99$), or family history ($\chi^2=0.0857$, $P=0.77$) between patients with keloids and healthy controls (**Table 1**). In the 990 patients with keloids, 273 patients (28%) had mild symptoms, 503 (51%) had moderate symptoms, and 214 (21%) had severe symptoms.

Genetic Associations Between Susceptibility to Keloids and GZMB Genetic Polymorphisms

All of the 15 candidate SNPs were included in the Hardy-Weinberg equilibrium tests in the control group, and the results are summarized in **Supplementary Table 1**. SNP rs8192917 was found to be significantly related with the susceptibility of keloids (**Table 2**). An increased risk of keloids was associated with the C allele (minor allele) of rs8192917 (odds ratio [OR]=1.33; 95%CI=1.18-1.49, $P=1.47\times 10^{-6}$). In addition to rs8192917, a couple of other SNPs achieved nominal significance despite their strong correlations with rs8192917 (**Figure 1**). A large LD block comprising 9 SNPs was constructed (**Figure 1**). Significant associations were obtained from multiple haplotypes within these LD blocks (**Table 3**, $\chi^2=329.60$, $P=2.81\times 10^{-67}$).

Genetic Associations for Clinical Severity of Keloids

A significant association was observed for genotypes of rs8192917 and clinical severity of keloids ($\chi^2=10.61$, $P=0.03$). The proportion of patients with TT genotypes (homozygote of major alleles) that had mild and severe symptoms was 26% and 10%, respectively. On the other hand, the proportion of patients with CC genotypes (homozygote of minor alleles) that had mild and severe symptoms was 24% and 17%, respectively (**Table 4**). The proportion of patients with mild symptoms was lower for patients with TT genotypes than for patients with CC genotypes, while the proportion of patients with severe symptoms was higher for patients with TT genotypes than for patients with CC genotypes. The copy number of the C allele was associated with more severe symptoms in patients with keloids.

Functional Consequences of SNP rs8192917

SNP rs8192917 is located in the exonic region of the *GZMB* gene. This SNP is a nonsynonymous variant, and its minor allele alters amino acids from Arg to Gln. Further bioinformatics tools were used to investigate whether this change in amino acids would in turn have significant functional consequences on proteins encoded by *GZMB*. The SIFT score was 0.189, and its prediction was “tolerated”. However, in Polyphen2, this SNP was predicted to be “possibly damaged”. Additionally, potential



Figure 1. Linkage disequilibrium structure of the 15 genotyped single nucleotide polymorphisms. Values of linkage disequilibrium are indicated in each cell. Linkage disequilibrium blocks are indicated in bold.

Table 3. Results of haplotype-based association analyses.

| Locus | SNPs | Haplotype | F_A | F_U | χ^2 | DF | P |
|-------|---|-----------|-------|-------|----------|----|------------------------|
| GZMB | rs2236338- rs6573910- rs6573911- rs71405867- rs1126639- rs11539752- rs10909625- rs10873219 | OMNIBUS | NA | NA | 329.60 | 7 | 2.81×10^{-67} |
| | | ACCAGGTG | 0.573 | 0.672 | 55.00 | 1 | 1.20×10^{-13} |
| | | GTTGACCT | 0.115 | 0.101 | 2.81 | 1 | 0.0936 |
| | | GTTGACCG | 0.048 | 0.058 | 2.12 | 1 | 0.1456 |
| | | GTTAACCT | 0.072 | 0.080 | 1.07 | 1 | 0.3017 |
| | | ACCAGGCG | 0.037 | 0.002 | 117.50 | 1 | 2.18×10^{-27} |
| | | ACTAGGTG | 0.081 | 0.038 | 48.52 | 1 | 3.26×10^{-12} |
| | | GTTAACCG | 0.032 | 0.048 | 7.36 | 1 | 0.0067 |
| | | GCCAGGTG | 0.042 | 0.002 | 137.30 | 1 | 1.01×10^{-31} |

F_A – haplotype frequency in patients with postsurgical keloids; F_U – haplotype frequency in controls; DF – degrees of freedom.

Table 4. Association between genotypes of rs8192917 and clinical severity of postsurgical keloids.

| Clinical severity (%) | Genotypes of SNP rs8192917 | | | χ^2 | P |
|-----------------------|----------------------------|------------|------------|----------|------|
| | TT (N=378) | CT (N=398) | CC (N=150) | | |
| Mild | 100 (26) | 137 (34) | 36 (24) | | |
| Moderate | 242 (64) | 198 (50) | 88 (59) | | |
| Severe | 36 (10) | 63 (16) | 26 (17) | 10.61 | 0.03 |

eQTL effects of this SNP on *GZMB* were also observed using the Genotype-Tissue Expression database. In tissue of the tibial nerve, a significant eQTL signal was observed (**Supplementary Figure 3**). The CC genotype of rs8192917 was significantly associated with a lower gene expression level of *GZMB*. Nevertheless, this eQTL signal was only identified in tissues of the tibial nerve, not in the other 45 kinds of human tissues, including the targeted tissue of keloids (**Supplementary Table 2**).

Discussion

Although multiple lines of evidence from studies of animal models have indicated that the *GZMB* gene might be involved in the pathogenesis mechanisms of keloids [21,22], few studies have been conducted to investigate the distribution of genetic polymorphisms of the *GZMB* gene in patients with keloids and controls. In our study, a significant association signal was identified between rs8192917 of *GZMB* and the susceptibility to keloids in the Chinese Han population. To the best of our knowledge, the present report is the first to validate this relationship in human populations. Several GWA studies have linked the *GZMB* gene to vitiligo [33,34], and a significant signal was also obtained from SNP rs8192917. Interestingly, even the effect directions reported in these previous GWA studies on vitiligo were the same as those in the present study on keloids. This observation suggests a potential common genetic basis between vitiligo and keloids, although very few studies on this topic have been conducted.

A previous study indicated that granzyme B (protein encoded by *GZMB*) inhibits the wound healing process by cleaving extracellular matrix proteins during chronic inflammation [19]. Furthermore, a recent study showed that serpin3n, which attenuates granzyme B-mediated decorin cleavage, can also accelerate the wound healing process in type II diabetic mice [20]. In this sense, if an allele of a SNP in the *GZMB* gene is related with increased susceptibility of keloids, the same allele should also be related to a lower expression of *GZMB* in relevant human tissues. Our findings agreed with this hypothesis. The minor allele (C allele) of rs8192917 was associated with increased susceptibility of keloids, and the CC genotype of rs8192917 was associated with a lower gene expression

level of *GZMB*. Additionally, we identified a significant association signal between the copy number of C alleles and the clinical severity of keloids in patients. This dosage-dependent pattern could also be considered evidence in support of the pathogenesis mechanism proposed here.

The functional consequence of SNP rs8192917 was reported inconsistently in SIFT and Polyphen2. The SIFT score was 0.189, and its prediction was “tolerated”. However, in Polyphen2, this SNP was predicted to be “possibly damaged”. This is not very surprising, and a recent report focusing on *BRCA1/2* has shown that due to low accuracies, current bioinformatics based tools might not be able to provide satisfying prediction results for variants with unknown significance [35]. Therefore, it is still too early to determine the functional consequence of this SNP solely based on in silico tools. Although this SNP was located at the exonic region and altered the amino acid in its encoded protein, it may only be a proxy for some ungenotyped susceptible DNA variants in the current report. Nevertheless, since *GZMB* is a relatively short gene and we genotyped all the common DNA variants, not just tag SNPs, we could deduce that those rare or low-frequency variants may be the ones that contribute to the risk and clinical severity of keloids. Furthermore, in the haplotype-based association analyses, a significant association signal was identified for haplotypes located within an LD block comprised of 9 SNPs. Although SNP rs8192917 was not included in this LD block, it was in strong LD with almost all 9 of its SNPs. Therefore, it was quite likely that this association signal obtained from haplotype analyses was dependent on rs8192917.

With the development of biotechnology, such as sequencing, genetic association analyses and multi-omics integrative analyses can help reveal the pathogenesis of complex diseases [36-39] and provide promising therapeutic candidates for the development of new drugs [40,41]. Therefore, sequencing-based integrative analysis might be a promising direction for determining the genetic architectures of *GZMB* on the susceptibility of keloids in the future.

It is worth mentioning the limitations of the present study. Although all common DNA variants located within the gene region of *GZMB*, including untranslated regions, were extracted, some key functional regions might still have been missed. The

10 kb to 15 kb regions upstream and downstream of a gene are considered to play important roles in gene expression regulation. However, in the present study, these regions were not scanned. In addition, necessary cautions are still needed in analyzing the eQTL signal observed from the publicly available database, because this signal was only identified in the tibial nerve, which is not a target tissue for keloids. Finally, this study had a small sample size, which might have affected the results.

Conclusions

The results of this study suggest there are significant associations between the common genetic variants in the *GZMB* gene and the susceptibility of postsurgical keloids in the Han

Chinese population. These genetic polymorphisms were also related with the severity of symptoms in participants with postsurgical keloids. The results of this study can contribute to future etiological and clinical research of keloids.

Acknowledgements

We would like to thank all the study participants for their cooperation.

Declaration of Figures' Authenticity

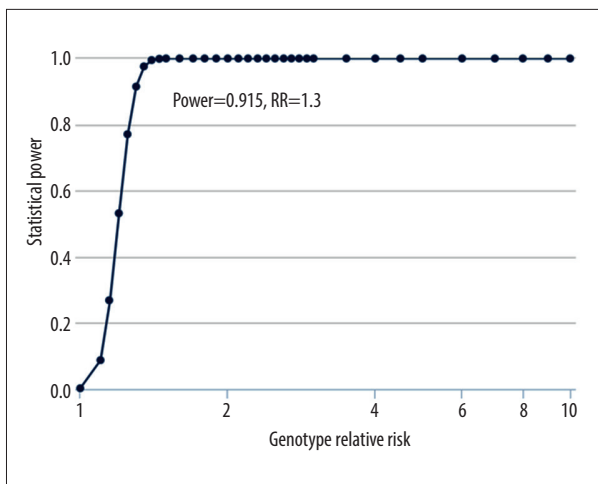
All figures submitted have been created by the authors, who confirm that the images are original with no duplication and have not been previously published in whole or in part.

Supplementary Materials

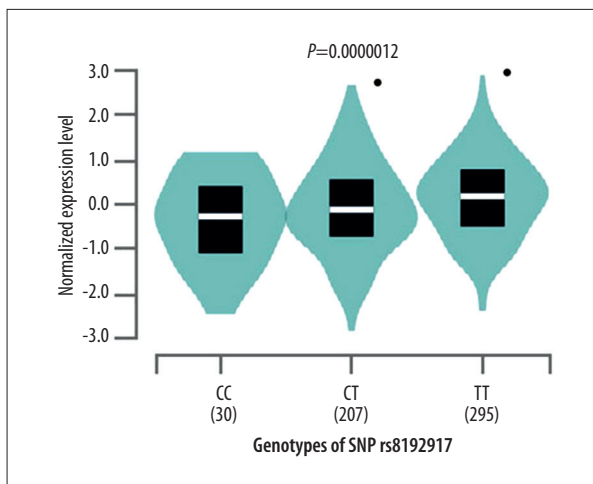
Supplementary Table 1. Basic information of the 15 genotyped SNPs.

| CHR | Position | SNP | A1 | A2 | Locus | Av Het | Av HetSE | FUNC | MAF | HWE |
|-----|----------|------------|----|----|-------|--------|----------|----------------|------|------|
| 14 | 24631041 | rs2236337 | C | T | GZMB | 0.369 | 0.220 | Untranslated-3 | 0.35 | 0.44 |
| 14 | 24631076 | rs2236338 | G | A | GZMB | 0.371 | 0.219 | Missense | 0.30 | 0.60 |
| 14 | 24631185 | rs74345106 | T | G | GZMB | 0.003 | 0.040 | Missense | 0.02 | 0.62 |
| 14 | 24631676 | rs6573910 | T | C | GZMB | 0.421 | 0.182 | Intron | 0.29 | 0.75 |
| 14 | 24631727 | rs6573911 | T | C | GZMB | 0.421 | 0.183 | Intron | 0.33 | 1.00 |
| 14 | 24632191 | rs71405867 | G | A | GZMB | 0.223 | 0.249 | Intron | 0.16 | 0.58 |
| 14 | 24632342 | rs1126639 | A | G | GZMB | 0.353 | 0.228 | Coding-synon | 0.29 | 0.60 |
| 14 | 24632383 | rs11539752 | C | G | GZMB | 0.369 | 0.220 | Missense | 0.29 | 0.96 |
| 14 | 24632423 | rs10909625 | C | T | GZMB | 0.362 | 0.224 | Codings-ynon | 0.29 | 0.87 |
| 14 | 24632500 | rs10873219 | T | G | GZMB | 0.319 | 0.240 | Intron | 0.18 | 0.56 |
| 14 | 24632691 | rs59268439 | T | C | GZMB | 0.113 | 0.209 | Intron | 0.12 | 0.92 |
| 14 | 24632850 | rs9671454 | C | G | GZMB | 0.332 | 0.236 | Intron | 0.04 | 0.18 |
| 14 | 24632954 | rs8192917 | C | T | GZMB | 0.377 | 0.215 | Missense | 0.29 | 0.55 |
| 14 | 24634203 | rs2273843 | C | T | GZMB | 0.259 | 0.250 | Untranslated-5 | 0.16 | 0.63 |
| 14 | 24634208 | rs2273844 | A | G | GZMB | 0.428 | 0.175 | Untranslated-5 | 0.29 | 1.00 |

CHR – chromosome; A1 – minor allele; A2 – major allele; avHet – average heterogeneity; avHetSE – standard error of average heterogeneity; FUNC – function; MAF – minor allele frequency; HWE – P values for Hardy-Weinberg equilibrium tests conducted in controls.



Supplementary Figure 1. Results of the power analysis for the present study.



Supplementary Figure 3. Violin plot for gene expression levels of GZMB in human tissue of tibial nerve grouped by genotypes of SNP rs8192917.



Supplementary Figure 2. The clinical characteristics of keloid scars and hypertrophic scars. (A) A 21-year-old man with postsurgical keloid scars. (B) A 24-year-old man with arm hypertrophic scars.

Supplementary Table 2. eQTL signals obtained for SNP rs8192917 on GZMB in 46 types of human tissues.

| Gene | SNP | P | NES | T-statistic | Tissue |
|------|-----------|-----------------------|--------|-------------|--------------------------------|
| GZMB | rs8192917 | 1.20×10 ⁻⁵ | 0.240 | 4.400 | Nerve – Tibial |
| GZMB | rs8192917 | 0.002 | 0.360 | 3.100 | Brain – Cerebellar Hemisphere |
| GZMB | rs8192917 | 0.006 | 0.130 | 2.800 | Adipose – Visceral (Omentum) |
| GZMB | rs8192917 | 0.008 | 0.054 | 2.600 | Whole Blood |
| GZMB | rs8192917 | 0.024 | 0.140 | 2.300 | Artery – Aorta |
| GZMB | rs8192917 | 0.032 | 0.160 | 2.200 | Liver |
| GZMB | rs8192917 | 0.035 | 0.140 | 2.100 | Pancreas |
| GZMB | rs8192917 | 0.040 | -0.110 | -2.100 | Skin – Sun Exposed (Lower leg) |
| GZMB | rs8192917 | 0.048 | 0.092 | 2.000 | Muscle – Skeletal |
| GZMB | rs8192917 | 0.064 | 0.240 | 1.900 | Brain – Substantia nigra |

Supplementary Table 2 continued. eQTL signals obtained for SNP rs8192917 on GZMB in 46 types of human tissues.

| Gene | SNP | P | NES | T-statistic | Tissue |
|------|-----------|-------|--------|-------------|---|
| GZMB | rs8192917 | 0.070 | 0.076 | 1.800 | Adipose – Subcutaneous |
| GZMB | rs8192917 | 0.074 | 0.079 | 1.800 | Esophagus – Mucosa |
| GZMB | rs8192917 | 0.090 | 0.140 | 1.700 | Spleen |
| GZMB | rs8192917 | 0.095 | 0.065 | 1.700 | Lung |
| GZMB | rs8192917 | 0.120 | 0.170 | 1.600 | Minor Salivary Gland |
| GZMB | rs8192917 | 0.130 | 0.074 | 1.500 | Stomach |
| GZMB | rs8192917 | 0.190 | 0.095 | 1.300 | Artery – Coronary |
| GZMB | rs8192917 | 0.190 | 0.160 | 1.300 | Cells – EBV-transformed lymphocytes |
| GZMB | rs8192917 | 0.200 | 0.100 | 1.300 | Pituitary |
| GZMB | rs8192917 | 0.210 | 0.073 | 1.200 | Esophagus – Muscularis |
| GZMB | rs8192917 | 0.260 | 0.059 | 1.100 | Breast – Mammary Tissue |
| GZMB | rs8192917 | 0.280 | 0.056 | 1.100 | Heart – Left Ventricle |
| GZMB | rs8192917 | 0.300 | 0.110 | 1.100 | Brain – Hypothalamus |
| GZMB | rs8192917 | 0.340 | -0.077 | -0.950 | Testis |
| GZMB | rs8192917 | 0.350 | 0.100 | 0.950 | Brain – Putamen (basal ganglia) |
| GZMB | rs8192917 | 0.370 | 0.054 | 0.890 | Skin – Not Sun Exposed (Suprapubic) |
| GZMB | rs8192917 | 0.390 | 0.065 | 0.850 | Adrenal Gland |
| GZMB | rs8192917 | 0.420 | 0.066 | 0.800 | Small Intestine – Terminal Ileum |
| GZMB | rs8192917 | 0.460 | 0.062 | 0.740 | Prostate |
| GZMB | rs8192917 | 0.490 | 0.067 | 0.700 | Brain – Caudate (basal ganglia) |
| GZMB | rs8192917 | 0.500 | -0.074 | -0.670 | Brain – Cortex |
| GZMB | rs8192917 | 0.580 | -0.064 | -0.560 | Vagina |
| GZMB | rs8192917 | 0.590 | -0.060 | -0.550 | Brain – Frontal Cortex (BA9) |
| GZMB | rs8192917 | 0.620 | 0.023 | 0.500 | Thyroid |
| GZMB | rs8192917 | 0.640 | -0.051 | -0.470 | Ovary |
| GZMB | rs8192917 | 0.660 | -0.059 | -0.450 | Uterus |
| GZMB | rs8192917 | 0.790 | 0.028 | 0.270 | Brain – Nucleus accumbens (basal ganglia) |
| GZMB | rs8192917 | 0.800 | -0.012 | -0.260 | Colon – Transverse |
| GZMB | rs8192917 | 0.800 | 0.013 | 0.250 | Heart – Atrial Appendage |
| GZMB | rs8192917 | 0.820 | 0.034 | 0.230 | Brain – Spinal cord (cervical c-1) |
| GZMB | rs8192917 | 0.840 | 0.014 | 0.200 | Colon – Sigmoid |
| GZMB | rs8192917 | 0.910 | 0.012 | 0.110 | Brain – Anterior cingulate cortex (BA24) |
| GZMB | rs8192917 | 0.930 | -0.012 | -0.090 | Brain – Amygdala |
| GZMB | rs8192917 | 0.940 | -0.003 | -0.073 | Artery – Tibial |
| GZMB | rs8192917 | 0.950 | 0.008 | 0.069 | Brain – Cerebellum |
| GZMB | rs8192917 | 0.980 | 0.003 | 0.030 | Brain – Hippocampus |

NES – normalized effect size. Threshold of *P* value was 0.05/46≈0.001.

References:

- Berman B, Maderal A, Raphael B. Keloids and hypertrophic scars: Pathophysiology, classification, and treatment. *Dermatol Surg.* 2017;43 Suppl. 1):S3-18
- Viera MH, Caperton CV, Berman B. Advances in the treatment of keloids. *J Drugs Dermatol.* 2011;10(5):468-80
- Satish L, Lyons-Weiler J, Hebda PA, Wells A. Gene expression patterns in isolated keloid fibroblasts. *Wound Repair Regen.* 2006;14(4):463-70
- Trace AP, Enos CW, Mantel A, Harvey VM. Keloids and hypertrophic scars: A spectrum of clinical challenges. *Am J Clin Dermatol.* 2016;17(3):201-23
- Ogawa R. Keloid and hypertrophic scars are the result of chronic inflammation in the reticular dermis. *Int J Mol Sci.* 2017;18(3):606
- Majumder A, Srivastava S, Ranjan P. Squamous cell carcinoma arising in a keloid scar. *Med J Armed Forces India.* 2019;75(2):222-24
- Kassi K, Kouame K, Kouassi A, et al. Quality of life in black African patients with keloid scars. *Dermatol Reports.* 2020;12(2):8312
- Olaitan PB. Keloids: Assessment of effects and psychosocial-impacts on subjects in a black African population. *Indian J Dermatol Venereol Leprol.* 2009;75(4):368-72
- Murao N, Seino K, Hayashi T, et al. Treg-enriched CD4+ T cells attenuate collagen synthesis in keloid fibroblasts. *Exp Dermatol.* 2014;23(4):266-71
- Chen Z, Zhou L, Won T, et al. Characterization of CD45RO(+) memory T lymphocytes in keloid disease. *Br J Dermatol.* 2018;178(4):940-50
- Le QU, Chun-Di HE, Dematology DO. [Research advances on genetic and related gene in keloid.] *China Medical Abstract of Dermatology.* 2015 [in Chinese]
- Wang CH, Shan MJ, Liu H, et al. Hyperbaric oxygen treatment on keloid tumor immune gene expression. *Chin Med J (Engl).* 2021;134(18):2205-13
- Rhett JM, Ghatnekar GS, Palatinus JA, et al. Novel therapies for scar reduction and regenerative healing of skin wounds. *Trends Biotechnol.* 2008;26(4):173-80
- Liu X, Gao J, Li X. [Experimental study on fas gene death domain mutations in keloid pedigrees.] *Zhongguo Xiu Fu Chong Jian Wai Ke Za Zhi.* 2007;21(7):698-701 [in Chinese]
- Liu YB, Liu XJ, Gao JH, Duan HJ. [Analysis of the sequence of the variant exon-8 of fibroblastic Fas gene in keloid.] *Chinese Journal of Clinical Rehabilitation.* 2006 [in Chinese]
- Velotti F, Barchetta I, Cimini FA, Cavallo MG. Granzyme B in inflammatory diseases: Apoptosis, inflammation, extracellular matrix remodeling, epithelial-to-mesenchymal transition and fibrosis. *Front Immunol.* 2020;11:587581
- Hiroyasu S, Hiroyasu A, Granville DJ, Tsuruta D. Pathological functions of granzyme B in inflammatory skin diseases. *J Dermatol Sci.* 2021;104(2):76-82
- Carrino DA, Mesiano S, Barker NM, et al. Proteoglycans of uterine fibroids and keloid scars: Similarity in their proteoglycan composition. *Biochem J.* 2012;443:361-68
- Hiebert PR, Boivin WA, Abraham T, et al. Granzyme B contributes to extracellular matrix remodeling and skin aging in apolipoprotein E knockout mice. *Exp Gerontol.* 2011;46(6):489-99
- Hsu I, Parkinson LG, Shen Y, et al. Serpina3n accelerates tissue repair in a diabetic mouse model of delayed wound healing. *Cell Death Dis.* 2014;5:e1458
- Heusel JW, Wesselschmidt RL, Shresta S, et al. Cytotoxic lymphocytes require granzyme B for the rapid induction of DNA fragmentation and apoptosis in allogeneic target cells. *Cell.* 1994;76(6):977-87
- Turner CT, Bolsoni J, Zeglinski MR, et al. Granzyme B mediates impaired healing of pressure injuries in aged skin. *NPJ Aging Mech Dis.* 2021;7(1):6
- Zhu F, Wu B, Li P, et al. Association study confirmed susceptibility loci with keloid in the Chinese Han population. *PLoS One.* 2013;8(5):e62377
- Bakry OA, Younes SF, Abdel Wahed M, et al. Evaluation of the role of granzyme B in exuberant scar pathogenesis: An immunohistochemical study. *Anal Quant Cytopathol Histopathol.* 2015;37(4):221-26
- Baryza M, Baryza G. The Vancouver Scar Scale: An administration tool and its interrater reliability. *J Burn Care Rehabil.* 1995;16:535-38
- Idriss N, Maibach H. Scar assessment scales: A dermatologic overview. *Skin Res Technol.* 2009;15(1):1-5
- Purcell S, Neale B, Todd-Brown K, et al. PLINK: A tool set for whole-genome association and population-based linkage analyses. *Am J Hum Genet.* 2007;81(3):559-75
- Barrett JC, Fry B, Maller J, Daly MJ. Haploview: Analysis and visualization of LD and haplotype maps. *Bioinformatics.* 2005;21(2):263-65
- Gabriel SB, Schaffner SF, Nguyen H, et al. The structure of haplotype blocks in the human genome. *Science.* 2002;296(5576):2225-29
- Vaser R, Adusumalli S, Leng SN, et al. SIFT missense predictions for genomes. *Nat Protoc.* 2016;11(1):1-9
- Adzhubei IA, Schmidt S, Peshkin L, et al. A method and server for predicting damaging missense mutations. *Nat Methods.* 2010;7(4):248-49
- Consortium GT. The Genotype-Tissue Expression (GTEx) project. *Nat Genet.* 2013;45(6):580-85
- Jin Y, Birlea SA, Fain PR, et al. Variant of TYR and autoimmunity susceptibility loci in generalized vitiligo. *N Engl J Med.* 2010;362(18):1686-97
- Jin Y, Andersen G, Yorgov D, et al. Genome-wide association studies of autoimmune vitiligo identify 23 new risk loci and highlight key pathways and regulatory variants. *Nat Genet.* 2016;48(11):1418-24
- Ernst C, Hahnen E, Engel C, et al. Performance of in silico prediction tools for the classification of rare BRCA1/2 missense variants in clinical diagnostics. *BMC Med Genomics.* 2018;11(1):35
- Guan F, Zhang T, Han W, et al. Relationship of SNAP25 variants with schizophrenia and antipsychotic-induced weight change in large-scale schizophrenia patients. *Schizophr Res.* 2020;215:250-55
- Zhang TX, Zhu L, Ni T, et al. Voltage-gated calcium channel activity and complex related genes and schizophrenia: A systematic investigation based on Han Chinese population. *J Psychiatr Res.* 2018;106:99-105
- Han W, Zhang TX, Ni T, et al. Relationship of common variants in CHRNA5 with early-onset schizophrenia and executive function. *Schizophr Res.* 2018;206:407-12
- Guan F, Ni T, Han W, et al. Evaluation of the relationships of the WBP1L gene with schizophrenia and the general psychopathology scale based on a case-control study. *Am J Med Genet B Neuropsychiatr Genet.* 2020;183:164-71
- Guan F, Ni T, Zhu W, et al. Integrative omics of schizophrenia: From genetic determinants to clinical classification and risk prediction. *Mol Psychiatry.* 2021;188:1-14
- Shen C, Li H, Li M, et al. DLRAPom: A hybrid pipeline of Optimized XGBoost-guided integrative multiomics analysis for identifying targetable disease-related lncRNA-miRNA-mRNA regulatory axes. *Brief Bioinform.* 2022;23(2):bbac046